

# Effect of Graft Modification with Poly(*N*-vinylpyrrolidone) on Thermal and Mechanical Properties of Poly(3-hydroxybutyrate-*co*-3-hydroxyvalerate)

Wei Wang,<sup>1,2</sup> Yu Zhang,<sup>1</sup> Meifang Zhu,<sup>1</sup> Yanmo Chen<sup>1</sup>

<sup>1</sup>State Key Laboratory for Modification of Chemical Fibers and Polymer Materials, Donghua University, Shanghai 201620, China

<sup>2</sup>Jiaxing University, Department of Textile Engineering, Zhejiang 314001, China

Received 17 September 2007; accepted 10 January 2008

DOI 10.1002/app.27983

Published online 24 April 2008 in Wiley InterScience (www.interscience.wiley.com).

**ABSTRACT:** Poly(*N*-vinylpyrrolidone) (PVP) groups were grafted onto poly(3-hydroxybutyrate-*co*-3-hydroxyvalerate) (PHBV) backbone to modify the properties of PHBV and synthesize a new novel biocompatible graft copolymer. The effect of graft modification with PVP on the thermal and mechanical properties of PHBV was investigated. The thermal stability of grafted PHBV was remarkably improved while the melting temperature ( $T_m$ ) was almost not affected by graft modification. The isothermal crystallization behavior of samples was observed by polarized optical microscopy and the results showed that the spherulitic radial growth rates ( $G$ ) of grafted PHBV at the same crystallization temperature ( $T_c$ ) decreased with increasing graft yield (graft%) of samples. Analysis of isothermal crystallization kinetics showed that both the surface free energy ( $\sigma_e$ )

and the work of chain-folding per molecular fold ( $g$ ) of grafted PHBV increased with increasing graft%, implying that the chains of grafted PHBV are less flexible than ungrafted PHBV. This conclusion was in agreement with the mechanical testing results. The Young's modulus of grafted PHBV increased while the elongation decreased with increasing graft%. The hydrophilicity of polymer films was also investigated by the water contact angle measurement and the results revealed that the hydrophilicity of grafted PHBV was enhanced. © 2008 Wiley Periodicals, Inc. *J Appl Polym Sci* 109: 1699–1707, 2008

**Key words:** graft copolymers; thermal properties; mechanical properties; poly(3-hydroxybutyrate-*co*-3-hydroxyvalerate) (PHBV); poly(*N*-vinylpyrrolidone) (PVP)

## INTRODUCTION

Poly(3-hydroxybutyrate-*co*-3-hydroxyvalerate) (PHBV), a thermoplastic aliphatic polyester synthesized by bacterial fermentation, is known to degrade fully in the environment without forming any toxic products. This biodegradable nature is very important from the view of reducing plastic wastes. The synthesis of PHBV is very different from common oil-based polymers. PHBV can be produced by microorganisms with renewable nature materials such as starch, waste edible oils, waste vegetable, waste fruit, and other organic wastes originated from industry and trade.<sup>1,2</sup> It can also be produced and extracted from plants, for example, *Arabidopsis*, through transgenic technology.<sup>3,4</sup> PHBV has many excellent properties such as biodegradability, biocompatibility, piezoelectric property, optical activity, and so on, and so it can be widely used as biodegradable packing materials, tissue engineering materials,

drug delivery system, and electric materials. With the shortage of energy resources and the growing concern for environmental protection in world, the exploration and application of PHBV is attracting more and more interests in research and industry fields.

The properties of PHBV can be tailored at a certain extent by varying the hydroxyvalerate (HV) contents of the copolymer. When the contents of HV are 3–8 mol %, the thermal and mechanical properties of PHBV are similar to polypropylene. PHBV can be processed in the melting state, and so it is a prospective substitute for currently used thermoplastic resin that is not biodegradable to alleviate the environmental crisis. However, the application of PHBV is very limited presently because of its inherent disadvantage such as high cost, hardness and brittleness, low thermal decomposition temperature, narrow heat-processing window, absence of functional groups, and so on. To improve the chemical, physical, and heating-processing properties of PHBV, various methods including chemical modification,<sup>5–8</sup> as well as blending with other polymers have been investigated.<sup>9–12</sup> Out of these modification methods, graft modification is a well-known method to modify the properties of the polymer as well as to introduce new functional groups to the same polymer back-

Correspondence to: W. Wang (zjxuwangwei@163.com).

Contract grant sponsor: Science and Technology Commission of Shanghai Municipality; contract grant number: 06JC14003.

bone. Many studies on the graft modification of PHBV have also been reported.<sup>13–18</sup>

Poly(*N*-vinylpyrrolidone) (PVP) is a synthetically derived vinyl polymer with a unique combination of properties, such as good solubility in water and a range of organic solvents, remarkable capacity to interact with a wide variety of organic and inorganic compounds, good biocompatibility, nontoxicity to living tissues, and so on. PVP has been widely used in the biomedical fields, the cosmetic and food industrial sectors which are closely related to the human health for decades. PVP has also been widely used as a medical additive or polymeric modifier.<sup>19–22</sup> Although there are several polymers or monomers that have been grafted onto PHBV, PVP has never been grafted onto it. If PVP could be grafted onto PHBV, not only the properties of PHBV could be improved but also new functional groups could be introduced. Meanwhile both substrate PHBV and grafted PVP side groups have biocompatibility, and so it is expected that the PHBV grafted with PVP also has biocompatibility. The products could be used as biomaterials and could be further functionalized to extend their application because PVP groups have the remarkable capacity to interact with a wide variety of organic and inorganic compounds.

The aim of our research was to synthesize a novel biocompatible graft copolymer that would combine the advantages of PHBV substrate and PVP side chains. In this article, the thermal stability and crystallization behavior of raw PHBV and grafted PHBV were investigated using thermogravimetric analysis (TGA), differential scanning calorimetry (DSC), polarized optical microscopy (POM), and wide-angle X-ray diffraction (WAXD). A remarkable effect of graft modification on the thermal properties of PHBV was detected. The molecular characteristic was investigated using gel permeation chromatography (GPC). The isothermal crystallization kinetics was analyzed according to nucleation theories. The mechanical properties and the hydrophilicity of graft copolymer films were also studied, as the graft copolymers are to be used as candidate biomaterials.

## EXPERIMENTAL

### Materials

PHBV (Hangzhou Tian'an Bioproducts, China; HV content: 3.57 mol %, determined by <sup>1</sup>H NMR spectrum) was recrystallized from ethanol. Grafted PHBV with PVP was synthesized in our laboratory as reported in the literature and the existence of chemical bond more likely the covalent bond between PVP groups and PHBV substrate has also been verified.<sup>23</sup> The parameter of graft yield (graft%)

used to express the PVP content in grafted PHBV products was defined as the following equation:

$$\text{graft}\% = 100W_{\text{PVP}}/W_{\text{PHBV}} \quad (1)$$

where  $W_{\text{PVP}}$  and  $W_{\text{PHBV}}$  represent the weight of PVP grafted onto PHBV substrate and the weight of PHBV substrate, respectively. To study the effect of graft modification on the properties of PHBV, samples with different graft% were selected. Grafted PHBV (2.54), grafted PHBV (6.98), grafted PHBV (9.01), and grafted PHBV (10.48) represent grafted PHBV with graft% of 2.54, 6.98, 9.01, and 10.48%, respectively.

### Measurements

GPC analysis was carried out with a PL-GPC50 Intogratad system equipped with a Waters pump and two Waters Styragel columns connected in series and a HP 1047 RI Hewlett-Packard refractive index detector. Chloroform was used as the eluent at a flow rate of 1.0 mL/min at 313 K. Monodispersed polystyrene standards were used to obtain a calibration curve. Samples were dissolved in chloroform at a concentration of 2.0 mg/mL and the injection volume was 100  $\mu$ L. Analyses lasted 25 min.

TGA was performed on a simultaneous analysis system (STA409PC, Germany) under nitrogen atmosphere at a heating rate of 20 K/min from 298 to 673 K. The sample weight was kept within 8–10 mg. The thermograms were obtained by plotting the percentage of residual mass against the temperature.  $T_{99\%}$  and  $T_{95\%}$  were defined as the temperature at which the percentage of residual mass was 99% and 95%, respectively.

DSC measurements were carried out on a Mettler-Toledo Star DSC822 System (Switzerland). The instrument was calibrated with an indium standard. The measurement was conducted under nitrogen atmosphere and the sample weight used in the DSC pan was kept within 6–8 mg. The samples were first heated up from room temperature to 463 K (first scan) at a rate of 20 K/min and then maintained at that temperature for 3 min to destroy all memories of the previous thermal and mechanic histories. They were then cooled down to room temperature (second scan) at a rate of 10 K/min and reheated up to 463 K (third scan) at the same rate.

The spherulitic growth and morphological structure of samples was observed with an Olympus BX51 POM equipped with a hot stage. Each specimen was sandwiched between two thin glass slides, kept at 463 K for 3 min on the hot stage, and then cooling down to a desired temperature ( $T_c$ ) as quickly as possible. The specimens were then isothermally crystallized at  $T_c$ . The growth rate of

**TABLE I**  
Molecular Characteristics of Ungrafted PHBV and Grafted PHBV

Samples	Graft%	$M_n$	$M_w (\times 10^5)$	$M_w/M_n$
Ungrafted PHBV	0	$6.03 \times 10^4$	2.45	4.06
Grafted PHBV(2.54)	2.54	$8.88 \times 10^4$	3.44	3.87
Grafted PHBV(6.98)	6.98	$1.20 \times 10^5$	3.78	3.15
Grafted PHBV(9.01)	9.01	$1.32 \times 10^5$	3.81	2.88
Grafted PHBV(10.48)	10.48	$1.43 \times 10^5$	4.11	2.88

spherulite radius was monitored as a function of time. The slope of the line obtained from a plot of the spherulitic radius versus time was taken as the spherulitic growth rate ( $G$ ).

WAXD experiments were performed with a Philips PW1700 X-ray diffractometer using Cu  $K\alpha$  X-rays at a voltage of 40 kV and a current of 30 mA.

PHBV and grafted PHBV films were prepared by casting 0.1 g/mL polymer solution in chloroform onto a glass dish. After slow evaporation of chloroform, the remaining solvent in the films was removed by drying the films in a high vacuum at 313 K for at least 24 h. Tensile properties of the dumbbell-shaped polymer films were carried out according to ASTM D 638-5 on an Instron (model 1211) mechanical testing machine at the standard atmosphere with a crosshead speed of 5 mm/min. The thickness of each specimen was determined by a digital micrometer and the average value of three different positions in specimen was adopted. The specimens were stored at the standard atmosphere for 2 weeks before testing. The values reported are the averages of at least 10 specimens.

Statistic water contact angles of the polymer films were measured by sessile drop method at the standard atmosphere using a contact angle goniometer (OCA20, Germany). The polymer films were prepared according to the method described earlier and the averaged thickness of each specimen determined by a digital micrometer was  $33 \pm 2 \mu\text{m}$ . For each contact angle reported, at least five readings from different parts of the film surface were averaged.

The surface analyses of polymer films were performed with a scanning electron microscope (JSM-5600LV, Nikon, Japan). The polymer films with thickness of  $33 \pm 2 \mu\text{m}$  were prepared as described earlier. Before the observation, the surfaces were coated with an Au-Pd alloy by using a scanning electron microscopy coating device.

## RESULTS AND DISCUSSION

### Molecular weights characterization

The molecular weights and molecular weight distributions of ungrafted PHBV and grafted PHBV were

determined by GPC. The influence of the graft% on the molecular characteristic of samples is shown in Table I. Both the number-average molecular weight ( $M_n$ ) and the weight-average molecular weight ( $M_w$ ) of samples increased. This may be caused by the hydrodynamic volume of macromolecule changes after graft modification. The molecular weight index ( $M_w/M_n$ ) decreases with increasing graft% of samples. This is probably due to the lower-molecular-weight PHBV macromolecule which is more easily attacked by radicals and can provide more graft sites in backbone. A typical GPC chromatogram for PHBV and grafted PHBV is shown in Figure 1. The observation of a unimodal peak in all GPC chromatograms indicates that the PVP homopolymer has been extracted completely. From the figure, it can be also seen that the GPC chromatograms of ungrafted PHBV and grafted PHBV have some overlapping areas, implying that some unreacted PHBV macromolecules remain in the products.

### Thermal stability analysis

The thermal stability of samples was evaluated with TGA. Figure 2 shows the relationship between the thermal stability and graft% of samples. Both  $T_{99\%}$  and  $T_{95\%}$  of samples increase with increasing graft%. The  $T_{99\%}$  and  $T_{95\%}$  of grafted PHBV (10.48) increased nearly 30 K by comparison with ungrafted PHBV, indicating that the thermal stability of grafted sample has been improved markedly which is very beneficial to the heat-processing. It is widely believed that the thermal degradation of PHBV occurs almost exclusively via a random chain scission mechanism involving a six-member ring transition state. The formation of six-member ring may be hindered by the side chains of PVP, and thus the thermal stability of grafted PHBV was improved.<sup>24,25</sup>

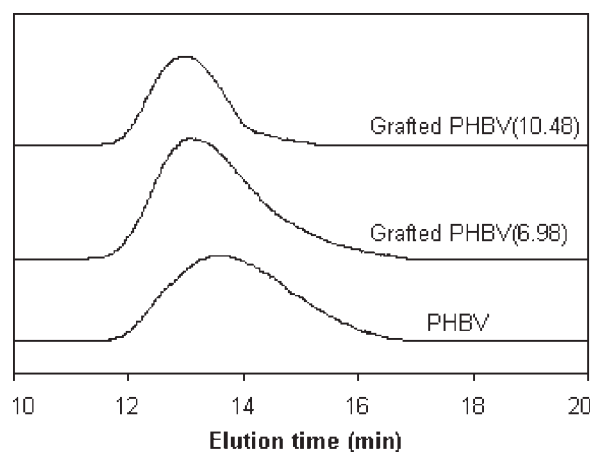


**Figure 1** The GPC curves of ungrafted PHBV and grafted PHBV.

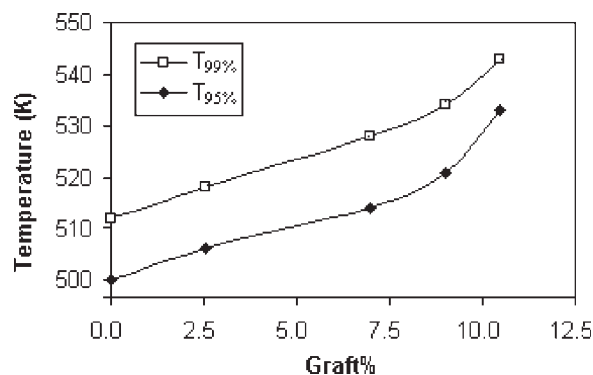


**Figure 2** The dependence of  $T_{99\%}$  and  $T_{95\%}$  on the graft% of samples.

### Thermal properties characterization

The thermal properties of samples were investigated by DSC. Figure 3 shows the DSC curves of samples on cooling (the second scan). The parameters derivable from the thermal analysis curves are summarized in Table II.  $T_{cc}$  is the peak temperature of crystallization on cooling. The onset-of-crystallization temperature,  $T_{cc(\text{onset})}$ , is the temperature at the intercept of tangents at the baseline and the high temperature side of exotherm peak. The parameter  $T_{cc(\text{onset})} - T_{cc}$  is a measure of the overall rate of crystallization. The smaller  $T_{cc(\text{onset})} - T_{cc}$  is, the higher is the crystallization rate.<sup>26</sup> The results show that both  $T_{cc}$  and  $T_{cc(\text{onset})}$  decrease while  $T_{cc(\text{onset})} - T_{cc}$  increases with increasing graft% of samples, indicating that the introduction of PVP side groups in PHBV backbone hinders the crystallization process and decreases the crystallization rate probably because of the steric effects for the regular fold of macromolecular chains.

Figure 4 shows the DSC curves of samples on heating (the third scan). It can be seen that there are two melting endothermic peaks on the curve of raw PHBV because of its unusual cocrystallization phenomena,<sup>27,28</sup> but only one peak appears in the curves of all grafted PHBV samples, indicating that the cocrystallization phenomena disappeared. It is of interest to note that a new exothermic peak appeared at almost the same temperature (323–324 K) in the DSC curves of all grafted PHBV samples regardless the different graft%. This new peak temperature is defined as  $T_{ch}$ , namely, the temperature at the crystallization exotherm peak upon heating. The appearance of  $T_{ch}$  is probably ascribed to recrystallization process of grafted PHBV upon heating because of its weakened crystallization ability upon cooling. The crystallization rate of raw PHBV upon cooling is relatively high, and so the crystallization process is mainly achieved before sample being cooled down to room temperature, but the crystallization rate of grafted PHBV is relatively low as mentioned earlier and the crystallization process could not be com-

pleted, and thus many imperfect spherulites and crystal nuclei would form upon cooling. These imperfect crystals and nuclei could not grow at low temperature. When the samples were heated up to a suitable temperature, these imperfect crystals and nuclei would grow again, and thus recrystallization happened and the new crystallization exothermic peak appeared.

The parameters derivable from Figure 4 are also summarized in Table II. The results show that the melting temperatures ( $T_m$ ) of all samples are almost unchanged. The enthalpy of crystallization on cooling ( $-\Delta H_{cc}$ ) decreases, while the enthalpy of recrystallization on heating ( $-\Delta H_{ch}$ ) increases with the increase in graft% of samples. This phenomenon is probably caused because of the fact that the lower the crystallization rate is, the more imperfect spherulites and crystal nuclei form on cooling, and thus the higher the recrystallization rate is and the more recrystallization enthalpy is on heating. Although the crystallization capability of grafted PHBV decreases with increasing graft%, the apparent enthalpy of fusion ( $\Delta H_f$ ) of all samples is almost constant, implying that the degree of crystallization is unchanged. This is probably due to the recrystallization process before melting of grafted PHBV on heating.

### Spherulitic morphology and structure

The spherulitic morphology of samples was observed with a POM. All the spherulites exhibit a typical banded structure with absence of cracks as shown in Figure 5. The band spacing changes with

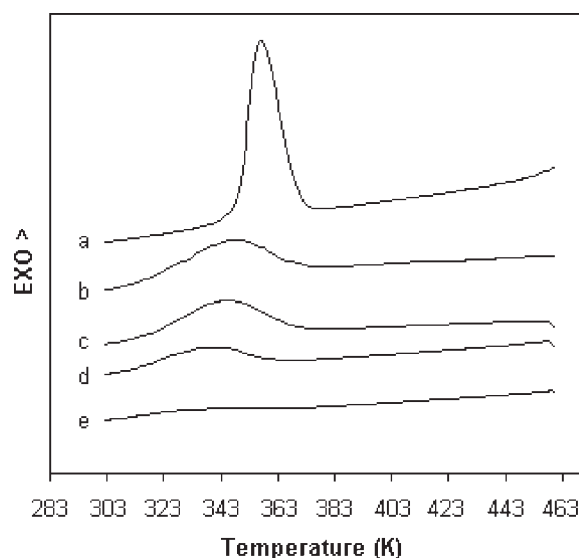


**Figure 3** The DSC curves of ungrafted PHBV and grafted PHBV on cooling (the second scan): (a) ungrafted PHBV, (b) grafted PHBV(2.54), (c) grafted PHBV(6.98), (d) grafted PHBV(9.01), (e) grafted PHBV(10.48).

TABLE II  
Thermal Parameters Derivable from DSC Traces of Ungrafted PHBV and Grafted PHBV

Samples	$T_{cc}$ (K)	$T_{cc(\text{onset})}$ (K)	$T_{cc(\text{onset})} - T_{cc}$ (K)	$-\Delta H_{cc}$ (J g <sup>-1</sup> )	$-\Delta H_{ch}$ (J g <sup>-1</sup> )	$T_m$ (K)	$\Delta H_f$ (J g <sup>-1</sup> )
Ungrafted PHBV	357.5	373.3	15.8	61.33	0 <sup>a</sup>	442.7 <sup>b</sup>	68.92
Grafted PHBV(2.54)	348.2	372.7	24.5	30.62	15.09	443.8	70.71
Grafted PHBV(6.98)	344.7	371.5	26.8	28.21	24.32	444.4	69.40
Grafted PHBV(9.01)	341.2	368.5	27.3	18.58	41.65	443.8	69.41
Grafted PHBV(10.48)	334.2	368.0	33.8	5.67 <sup>c</sup>	50.04	443.3	68.47

<sup>a</sup> No crystallization exotherm peak appeared.

<sup>b</sup> The higher peak temperature.

<sup>c</sup> Peak can be obtained from the enlarged DSC trace.

isothermal crystallization temperature ( $T_c$ ) and graft%. For the same sample, the band spacing decreases with the decrease of  $T_c$ . At a given  $T_c$ , the band spacing decreases with the increase in graft%. Generally, the banded structure of spherulite is due to the existence of twisted lamellae resulting from stress build up during crystallization and probably occurring within disordered fold surfaces of polymer crystals.<sup>29,30</sup> Hence, one possible explanation for this band spacing change of the spherulites is that the presence of PVP side chains and the decrease in  $T_c$  will give rise to the stress on the lamellar surfaces of samples.

Studies on the structure of crystals were carried out with WAXD. The WAXD results are shown in Figure 6. When the spectra of ungrafted PHBV are compared with those of the grafted PHBV, we can see that the  $d$ -spacing values is constant for the (020), (110), and (111) crystallographic planes, indicating that the crystalline unit cell of all samples is

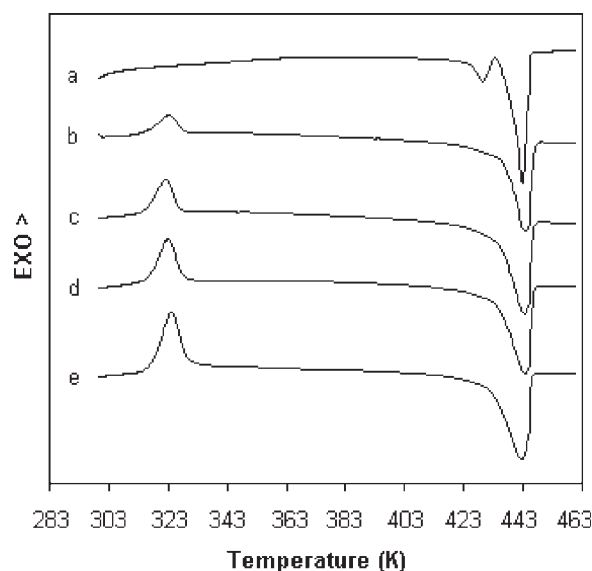


**Figure 4** The DSC curves of ungrafted PHBV and grafted PHBV on heating (the third scan): (a) ungrafted PHBV, (b) grafted PHBV(2.54), (c) grafted PHBV(6.98), (d) grafted PHBV(9.01), (e) grafted PHBV(10.48).

not changed. Furthermore, the intensity of all characteristic peaks for each sample is not changed obviously, indicating that the crystallization degree of samples is almost constant.

### Spherulitic growth analysis

In this work, the spherulitic radial growth rates ( $G$ ) of raw PHBV and grafted PHBV isothermally crystallized at different temperature ( $T_c$ ) were determined by using POM. The spherulitic radius was monitored as a function of time and the slope of the

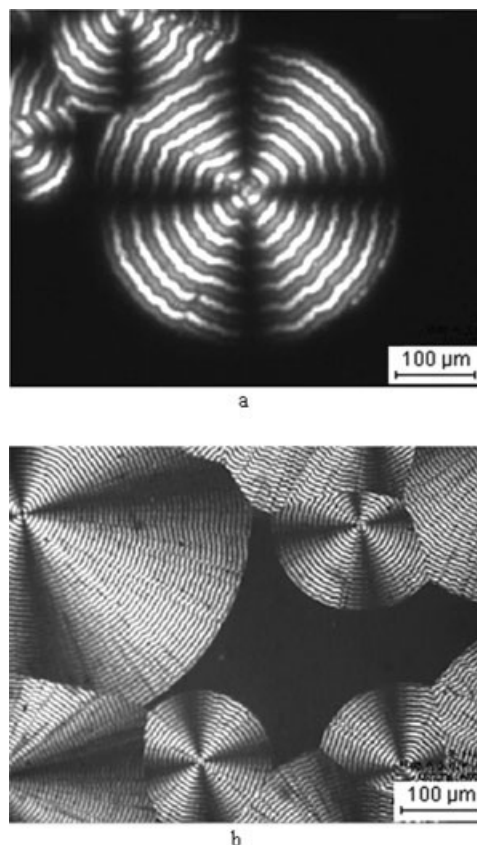


**Figure 5** The polarized optical micrographs of samples isothermally crystallized at 358 K: (a) ungrafted PHBV, (b) grafted PHBV(9.01).

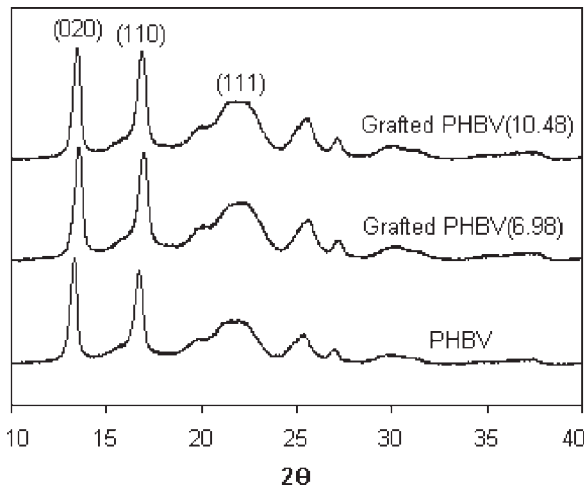


**Figure 6** The WAXD patterns of ungrafted PHBV and grafted PHBV.

line obtained from a plot of the spherulitic radius versus time was taken as the  $G$  value. The dependence of  $G$  of samples on  $T_c$  is shown in Figure 7. The range of  $T_c$  was from 338 to 373 K. From the figure, it can be seen that the  $G$  values of all samples reach a maximum at a certain crystallization temperature ( $T_{max}$ ). For ungrafted PHBV, the  $T_{max}$  is at about 363 K, while the  $T_{max}$  of grafted PHBV shifts to lower temperatures as the graft% increases. In addition, the  $G$  values of grafted PHBV samples decrease with increasing graft% at the same  $T_c$ , indicating that the presence of PVP side groups reduces the  $G$  values of grafted PHBV samples. This was probably caused by the decrease of segmental mobility for grafted PHBV because of the steric effects of PVP side chains.

The kinetic theory of polymer crystallization may be used to analyze the  $G$  data and obtain values for surface energies within the crystals. The radial growth rate of spherulites may be described by the famous Lauritzen–Hoffman equation as

$$G = G_o \exp[-U^*/R(T_c - T_\infty)] \exp[-K_g/(T_c \Delta T)] \quad (2)$$

where  $G_o$  is a constant,  $-U^*$  is the activation energy for transport of crystallizable segments through the melt to the site of crystallization,  $R$  is the gas constant,  $T_\infty$  is a hypothetical temperature below which all molecules become immobile,  $\Delta T$  is the degree of supercooling, and  $\Delta T = T_m^0 - T_c$ ,  $T_m^0$  is equilibrium melting point,  $K_g$  is the nucleation constant and can be expressed as

$$K_g = nb_o\sigma\sigma_e T_m^0 / (\Delta H_f^0 k) \quad (3)$$

where  $b_o$  is the molecular thickness,  $\sigma$  and  $\sigma_e$  are the lateral and surface free energies of the growing crystal, respectively,  $\Delta H_f^0$  is the heat of fusion per unit

volume of a perfect crystal, and  $k$  is Boltzmann's constant.  $n$  may have the value 2 or 4, depending on the relative rates of secondary nucleation and spreading along the growth front of the crystal. It is most convenient to rearrange eq. (2) as

$$\ln G + U^*/[R(T_c - T_\infty)] = \ln G_o - K_g/(T_c \Delta T) \quad (4)$$

A plot of  $\ln G + U^*/[R(T_c - T_\infty)]$  against  $1/(T_c \Delta T)$  should yield a straight line with an intercept  $\ln G_o$  and slope  $-K_g$  according to eq. (4). To do this we need to know the values of  $U^*$ ,  $T_\infty$ , and  $T_m^0$ . Here, for convenience of calculation, the data,  $U^* = 10.25$  kJ/mol,  $T_\infty = 225$  K, and  $T_m^0 = 448$  K, for PHBV containing 7 mol % HV reported in the literature were adopted.<sup>31</sup> Thus such plots were obtained (Fig. 8). From the figure it can be seen that the data give a reasonable straight line and yield  $K_g$  value of the samples.

The derived  $K_g$  can be used to calculate the surface free energy  $\sigma_e$  by using eq. (3). Here, for convenience of calculation, the data,  $n = 4$ ,  $b_o = 5.8 \times 10^{-10}$  m,  $\Delta H_f^0 = 1.65 \times 10^8$  J/m<sup>3</sup>, and  $\sigma = 2.55 \times 10^{-2}$  J/m<sup>2</sup>, reported in the literature for PHBV containing 7 mol % HV were adopted.<sup>31,32</sup>

The work of chain folding per molecular fold ( $q$ ) can be obtained by the following equation:

$$q = 2N_A a_o b_o \sigma_e \quad (5)$$

where  $N_A$  is Avogadro constant and  $a_o$  presents the molecular width. Here, the value  $a_o = 6.6 \times 10^{-10}$  m was adopted according to the literature.<sup>32</sup>

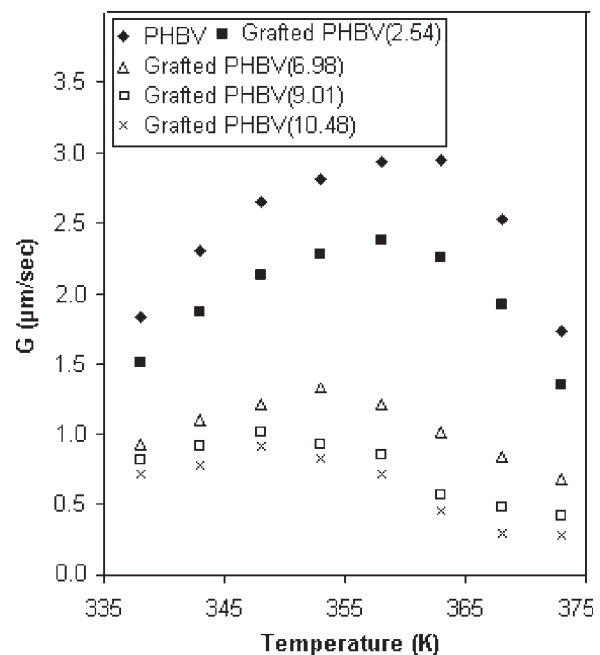


**Figure 7** The radial growth rate ( $G$ ) of spherulites isothermally crystallized at different  $T_c$ .

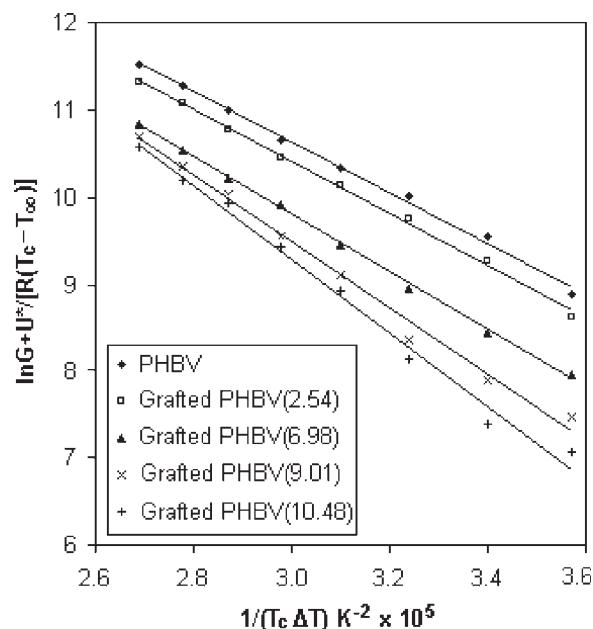


**Figure 8** Plots of  $\ln G + U^*/[R(T_c - T_\infty)]$  versus  $1/(T_c \Delta T)$  for ungrafted PHBV and grafted PHBV.

The resulting  $K_g$ ,  $\sigma_e$ , and  $q$  are listed in Table III. The values of  $K_g$ ,  $\sigma_e$ , and  $q$  increase with increasing graft% of samples, indicating that the crystallization of grafted PHBV with higher graft% becomes more difficult. This result is in agreement with those from DSC scans in the cooling and heating modes, as already mentioned. Moreover, the increase in  $q$  values means that the chains of grafted PHBV are less flexible than those of ungrafted PHBV. This is expected because the segmental mobility of grafted PHBV decreases due to the steric effects of PVP side groups. The more inflexible properties of grafted PHBV will be further verified by tensile testing.

### Mechanical properties

Figure 9 shows the typical stress–strain curves of ungrafted PHBV and grafted PHBV films. All specimens fail in a brittle manner, implying that the brittleness and hardness of PHBV has not been changed

**TABLE III**  
 $K_g$ ,  $\sigma_e$ , and  $q$  Values for Ungrafted PHBV and Grafted PHBV

Samples	$K_g$ ( $\times 10^5$ K <sup>2</sup> )	$\sigma_e$ ( $\times 10^{-2}$ J m <sup>-2</sup> )	$q$ (kJ mol <sup>-1</sup> )
Ungrafted PHBV	2.91	2.50	11.52
Grafted PHBV(2.54)	2.98	2.56	11.80
Grafted PHBV(6.98)	3.33	2.86	13.19
Grafted PHBV(9.01)	3.83	3.29	15.17
Grafted PHBV(10.48)	4.24	3.64	16.79

in essence after graft modification. During the tension procedure, the stress-whitening and development of transverse craze-like cracks were observed for all specimens. No neck appeared upon tension, and only universal narrowing with nearly constant volume was observed. After fracture, the elongated specimens gradually shrank to their original size. All these phenomena support that crazing is the main fracture mechanism for all specimens.

Table IV summarizes the tensile properties of ungrafted PHBV and grafted PHBV films. The Young's modulus of polymer films increases while the elongation at break decreases and the tensile strength is almost not changed with increasing the graft% of samples. The increase in Young's modulus and decrease in elongation indicates that the grafted PHBV films are more brittle than ungrafted PHBV. This is probably caused by the less flexible properties of grafted PHBV chains because of the steric effects of PVP side groups as described earlier.

### Hydrophilicity

The surface hydrophilicity of polymer films, as characterized by the static water contact angle, is shown in Figure 10. The water contact angle of grafted PHBV decreases with increasing graft%, indicating that the surface hydrophilicity is enhanced through incorporation of the PVP side chains. The enhanced hydrophilicity of grafted PHBV is due to the fact that the PVP is a polar macromolecule and has good solubility in water.

### Surface morphology

Figure 11 shows the surface morphology of ungrafted PHBV and grafted PHBV(10.48) films. All the morphological features show a one-phase behavior. This is because that the reaction of grafting PVP

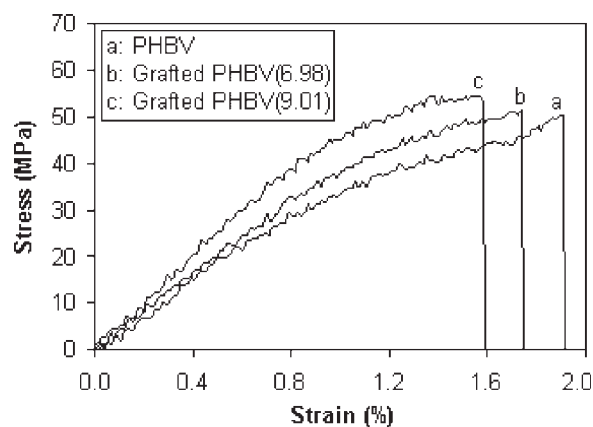


**Figure 9** The stress–strain curves of polymer films.

TABLE IV  
Tensile Properties of Polymer Films

Samples	Young's modulus (GPa)	Elongation at break (%)	Tensile strength (MPa)
Ungrafted PHBV	$3.18 \pm 0.12$	$1.91 \pm 0.08$	$50.51 \pm 3.58$
Grafted PHBV(2.54)	$3.42 \pm 0.23$	$1.84 \pm 0.12$	$52.03 \pm 4.21$
Grafted PHBV(6.98)	$3.92 \pm 0.26$	$1.74 \pm 0.10$	$51.52 \pm 3.16$
Grafted PHBV(9.01)	$4.13 \pm 0.15$	$1.69 \pm 0.06$	$53.07 \pm 2.90$
Grafted PHBV(10.48)	$4.28 \pm 0.31$	$1.57 \pm 0.13$	$54.59 \pm 4.03$

onto PHBV backbone was a kind of homogeneous solution polymerization.<sup>23</sup> However, the surface morphology of grafted PHBV(10.48) shows an increase of porosity and decrease of smooth, which is probably due to the fact that the viscosity of grafted PHBV(10.48) solution in chloroform was higher than ungrafted PHBV at the same polymer concentration because of the increased molecular weight.

### CONCLUSIONS

Potentially biocompatible graft copolymers (grafted PHBV with PVP) with various graft% have been successfully synthesized. Their molecular characteristics were studied with GPC. The results indicated that the grafted PHBV had higher molecular weights and narrower molecular weight distributions with increasing graft%. The thermal stability of samples was measured by TGA and the results showed that grafted PHBV presented better thermal stability with increasing graft%, which is very beneficial to the heat-processing. The DSC cooling traces of samples showed that the  $T_{cc}$  and  $T_{cc(\text{onset})}$  of grafted PHBV decreased, while the value of  $T_{cc(\text{onset})} - T_{cc}$  increased with increasing graft% of samples, indicating that the crystallization ability and crystallization rate of grafted PHBV decreased with the increase of

graft%. The  $T_m$  of samples was not affected by graft modification, but a new exothermic crystallization peak ( $T_{ch}$ ) appeared at almost the same temperature in the DSC heating curves of all grafted PHBV samples. Although the crystallization capability of grafted PHBV decreased, the apparent enthalpy of fusion ( $\Delta H_f$ ) of all samples was almost constant, implying that the degree of crystallization was unchanged. The structure of crystals was studied with WAXD and the results showed that the crystal structure and crystallization degree of all samples were almost not changed. The isothermally crystallized spherulitic morphology and growth rate ( $G$ ) were observed with a POM. All the spherulites exhibited a typical banded structure without cracks,

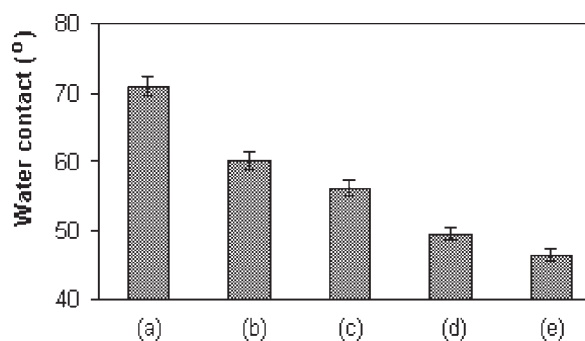


Figure 10 The static water contact angles of ungrafted PHBV and grafted PHBV films: (a) ungrafted PHBV, (b) grafted PHBV(2.54), (c) grafted PHBV(6.98), (d) grafted PHBV(9.01), (e) grafted PHBV(10.48).

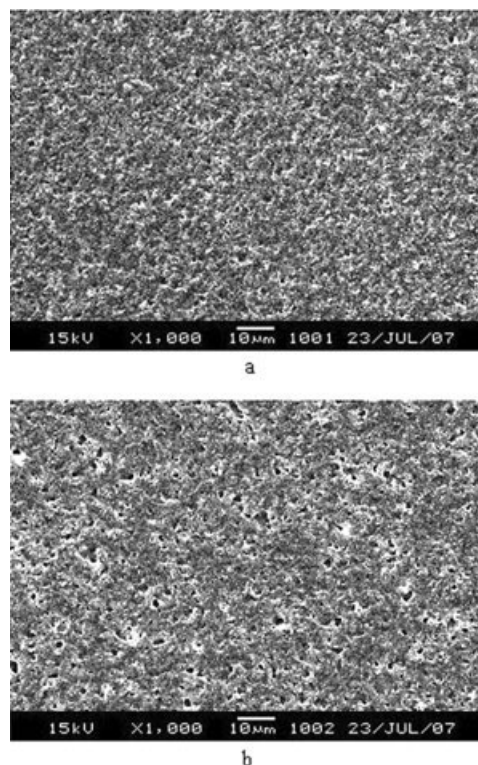


Figure 11 The surface morphology of polymer films as determined by SEM: (a) ungrafted PHBV, (b) grafted PHBV(10.48).



but the presence of PVP side groups decreased the band spacing and radial growth rate of spherulites at the same  $T_c$ . The  $T_{max}$  of grafted PHBV also shifted to a lower temperature. These results further indicated that the crystallization process of grafted PHBV was restricted. Analysis of spherulitic radial growth according to nucleation theories showed that both the surface free energy ( $\sigma_e$ ) and the work of chain folding per molecular fold ( $q$ ) of grafted PHBV increased with increasing graft%, implying that the chains of grafted PHBV were less flexible than ungrafted PHBV. This conclusion was in agreement with the mechanical testing results. The Young's modulus of grafted PHBV increased while the elongation decreased with increasing graft%, implying that the hardness and brittleness of raw PHBV could not be modified by graft modification. Through incorporation of PVP side chains, the surface hydrophilicity of grafted PHBV was improved, as revealed by water contact measurement, while the surface morphology of all polymer films showed a homogeneous phase behavior as determined by SEM.

## References

- Chen, C. W.; Don, T. M.; Yen, H. F. *Process Biochem* 2006, 41, 2289.
- Taniguchi, I.; Kagotani, K.; Kimura, Y. *Green Chem* 2003, 5, 545.
- Slater, S.; Mitsky, T. A.; Houmiel, K. L.; Hao, M.; Gruys, K. J. *Nat Biotechnol* 1999, 17, 1011.
- Ye, L.; Wang, T.; Song, Y. R. *Chin Sci Bull* 1999, 44, 1729.
- Guerrouani, N.; Baldo, A.; Maarouf, T.; Belu, A. M.; Mas, A. *J Fluorine Chem* 2007, 128, 925.
- Haene, P. D.; Remsen, E. E.; Asrar, J. *Macromolecules* 1999, 32, 5229.
- Gursel, I.; Balcik, C.; Arica, Y.; Akkus, O.; Akkas, N.; Hasirci, V. *Biomaterials* 1998, 19, 1137.
- Fei, B.; Chen, C.; Chen, S.; Peng, S. W.; Zhuang, Y. G.; An, Y. X.; Dong, L. S. *Polym Int* 2004, 53, 937.
- Li, J.; Lai, M. F.; Liu, J. J. *J Appl Polym Sci* 2005, 98, 1427.
- Ferreira, B. M. P.; Zavaglia, C. A. C.; Duek, E. A. R. *J Appl Polym Sci* 2002, 86, 2898.
- Shibata, M.; Oyamada, S.; Kobayashi, S. I.; Yaginuma, D. *J Appl Polym Sci* 2004, 92, 3857.
- Tan, S. M.; Ismail, J.; Kummerlöwe, C.; Kammer, H. W. *J Appl Polym Sci* 2006, 101, 2776.
- Tesema, Y.; Raghavan, D.; Stubbs, J., III. *J Appl Polym Sci* 2004, 93, 2445.
- Hu, S. G.; Jou, C. H.; Yang, M. C. *J Appl Polym Sci* 2003, 88, 2797.
- Hu, S. G.; Jou, C. H.; Yang, M. C. *Biomaterials* 2003, 24, 2685.
- Park, J.; Park, J. G.; Choi, W. M.; Ha, C. S.; Cho, W. J. *J Appl Polym Sci* 1999, 74, 1432.
- Ke, Y.; Wang, Y. J.; Ren, L.; Lu, L.; Wu, G.; Chen, X. F.; Chen, J. D. *J Appl Polym Sci* 2007, 104, 4088.
- Tesema, Y.; Raghavan, D.; Stubbs, J., III. *J Appl Polym Sci* 2005, 98, 1916.
- Devi, A. D.; Smitha, B.; Sridhar, S.; Aminabhavi, T. M. *J Membrane Sci* 2006, 280, 45.
- Caykara, T.; Alaslan, A.; Eroglu, M. S.; Guven, O. *Appl Surf Sci* 2006, 252, 7430.
- Cook, S. E.; Park, I. K.; Kim, E. M.; Jeong, H.; Akaike, T.; Cho, C. S. *J Controlled Release* 2005, 105, 151.
- Källrot, M.; Edlund, U.; Albertsson, A. C. *Biomaterials* 2006, 27, 1788.
- Wang, W.; Zhang, Y.; Chen, Y. M. *Iran Polym J* 2007, 16, 195.
- Grassie, N.; Murray, E. J.; Holmes, P. A. *Polym Degrad Stab* 1984, 6, 127.
- Lehrle, R.; Williams, R.; French, C. *Macromolecules* 1995, 28, 4408.
- Li, J.; Lai, M. F.; Liu, J. J. *J Appl Polym Sci* 2004, 92, 2514.
- Scandola, M.; Ceccorulli, G.; Pizzoli, M.; Gazzano, M. *Macromolecules* 1992, 25, 1405.
- Bluhm, T. L.; Hamer, G. K.; Marchessault, R. H.; Fyfe, C. A. *Macromolecules* 1986, 19, 2871.
- Xing, P. X.; Dong, L. S.; An, Y. X.; Feng, Z. L. *Macromolecules* 1997, 30, 2726.
- Fei, B.; Chen, C.; Wu, S.; Peng, S. W.; Wang, X. Y.; Dong, L. S.; Xin, J. H. *Polymer* 2004, 45, 6275.
- Organ, S. J.; Barham, P. J. *J Mater Sci* 1991, 26, 1368.
- Peng, S. W.; An, Y. X.; Chen, C.; Fei, B.; Zhang, Y. G.; Dong, L. S. *Eur Polym J* 2003, 39, 1475.